Tau Polymerization: Role of the Amino Terminus[†]

T. Chris Gamblin, Robert W. Berry, and Lester I. Binder*

Department of Cell and Molecular Biology and Cognitive Neurology and Alzheimer's Disease Center, Feinberg School of Medicine, Northwestern University, Chicago, Illinois 60611-3008

Received November 27, 2002; Revised Manuscript Received January 9, 2003

ABSTRACT: The abnormal polymerization of the tau molecule into insoluble filaments is a seminal event in the neurodegenerative process underlying Alzheimer's disease. Previous experimentation has shown that the microtubule-binding repeat region of the molecule is vital for its ability to polymerize in vitro into filaments similar to those found in Alzheimer's disease. However, it is becoming clear that regions outside the microtubule-binding repeat, such as exons 2 and 3 and the carboxy-terminal tail, can greatly influence its polymerization. Since it has been previously postulated that the amino terminus of tau could be involved in generating pathological conformations in the disease state, its role in the polymerization process was investigated. This report demonstrates that the removal of the amino terminus greatly inhibits the polymerization of the tau molecule, reducing both the rate and extent of polymerization. These results support the hypothesis that the ability of tau to form specific conformations involving the amino terminus is an early event in the formation of tau polymers in the disease state. Furthermore, the mutation of arginine 5 to leucine ($^{R}5^{L}$), mimicking an amino-terminal tau mutation found in a single case of FTDP-17, enhances the polymerization of the tau molecule. Therefore, the amino terminus of the tau molecule, while largely overlooked in studies of its polymerization, is a significant contributor to the polymerization process.

The polymerization of the microtubule-associated protein tau into insoluble filaments is a significant event in the progression of certain forms of neurodegeneration (reviewed in ref *1*). It has been shown that increases in the amount of tau deposition in specific brain regions correlate well with the nature and extent of cognitive decline in Alzheimer's disease (*2*). In fact, mutations in the tau gene cause a decreased affinity for microtubules and/or an increased propensity for self-aggregation in vitro. It is postulated that these changes lead to increased tau pathology in situ and are likely responsible for the observed neurofibrillary degeneration in hereditary frontotemporal dementia and Parkinsonism linked to chromosome 17 (FTDP-17)[1] (reviewed in ref *1*).

It is therefore of some importance to understand what changes in the tau molecule can lead to its transformation into a pathological entity, as such knowledge could potentially lead to the development of therapeutic strategies. To that end, much effort has been expended in modeling the polymerization of tau in vitro, where this event can be carefully controlled to study the underlying biochemical and biophysical parameters that govern the process. Although tau protein can self-aggregate under near-physiological conditions (*3*), it has been shown that the polymerization of recombinant tau protein can be enhanced through the addition of various inducer molecules. Examples of inducer molecules include polyanionic compounds such as heparin (*4*−*10*), nucleic acids (*11*), and polyglutamate (*5*), as well as polyunsaturated fatty acids such as arachidonic acid (*9*, *12*−*17*), docosahexaenoic acid (*15*), or possibly some oxidative variant of these fatty acids (*15*).

Previous work has shown that truncation of the tau molecule can greatly enhance its rate of polymerization. In fact, it has been shown that a portion of the microtubule-binding repeat region as short as six amino acids is capable of self-aggregation in the presence of polyanionic compounds (*18*). In the presence of fatty acids, it has been shown that the truncation of tau at its carboxyl terminus increases the rate and extent of its polymerization (*17*). However, the involvement of the amino terminus in the polymerization reaction has yet to be investigated. The amino terminus is believed to be important in the generation of tau pathology since it has been shown that it comes in close proximity to the microtubule-binding repeat (MTBR) region to form the discontinuous Alz50 epitope (*19*−*21*). Since Alz50 reactivity can be observed in pretangle neurons (*22*), the adoption of this conformation is postulated to be an early step in the generation of pathological forms of tau. With the recent discovery of a case of frontotemporal dementia and Parkinsonism linked to chromosome 17 (FTDP-17) bearing a mutation in the amino-terminal region of the tau molecule (Arg 5 to Leu, $^{R}5^{L}$) (*23*), it became imperative that this region of the molecule be examined.

In the current study, we have found that the removal of the amino-terminal portion of the Alz50 epitope inhibits the fatty acid induction of tau polymerization in vitro. Given the striking results of this amino-terminal modification, we

[†] Supported by NIH Grants AG14453 (L.I.B.) and NS11040 (T.C.G.).

* To whom correspondence should be addressed. Tel: (312) 503-0823. Fax: (312) 503-7912. E-mail: l-binder@northwestern.edu.

[1] Abbreviations: MTBR, microtubule-binding repeats; FTDP-17, frontotemporal dementia and Parkinsonism linked to chromosome 17; HEPES, *N*-(2-hydroxyethyl)piperazine-*N*′-2-ethanesulfonic acid; DTT, dithiothreitol; i_s, intensity of scattered light.

10.1021/bi0272510 CCC: $25.00
Published on Web 01/31/2003

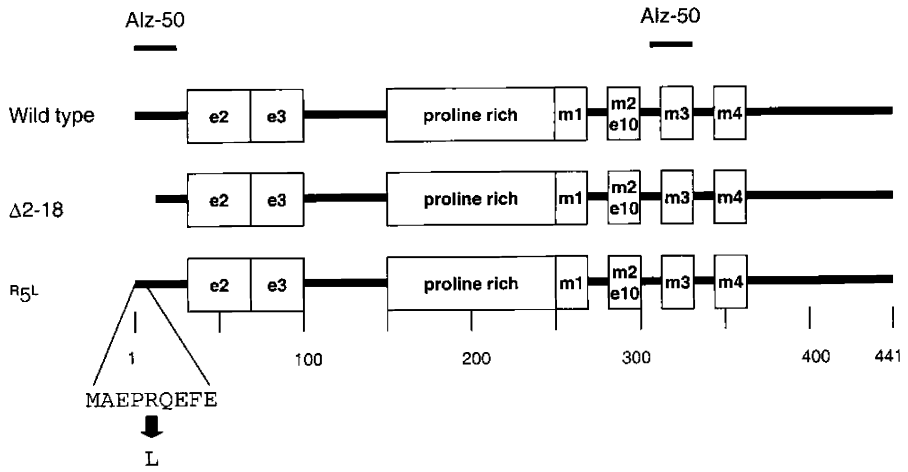

FIGURE 1: Schematic of constructs employed. Line diagrams are shown for the three constructs employed here. The longest isoform of tau found in the central nervous system is referred to as wild type and served as the control for the experiments. The different regions of the molecule are depicted as boxes and are exon 2, exon 3, the proline-rich region, and microtubule-binding repeats 1−4. In addition, the regions of the molecule corresponding to the discontinuous Alz50 epitope are depicted. The second construct is the Δ2−18 mutant, which is lacking amino acids 2−18. The third construct is $^{R}5^{L}$, and the sequence containing the mutation is depicted.

also modeled the effects of the $^{R}5^{L}$ tau mutation. The $^{R}5^{L}$ mutation results in a rapid increase in tau polymerization in the presence of arachidonic acid, indicating a potential toxic gain of function for the mutation. These results suggest a new role for the amino terminus of tau in its polymerization in neurodegenerative diseases.

EXPERIMENTAL PROCEDURES

Chemicals and Proteins. Full-length human tau protein (2N4R htau) and the Δ2−18 mutant were expressed in *Escherichia coli* and purified as described previously (*21*). Arachidonic acid (AA) was purchased from Cayman Chemicals (Ann Arbor, MI) and stored at −20 °C. To control for possible oxidation during storage, the fatty acids were used for a short time (less than 3 months) and then discarded. The peptide corresponding to amino acids 1−15 (MAEPRQEFEVMEDHA) was synthesized and purified to 95% purity by Cell Essentials, Inc. (Boston, MA).

Site-Directed Mutagenesis. The $^{R}5^{L}$ mutation in 2N4R htau was prepared from pT7c-htau40 using a commercial kit (QuickChange, Stratagene, La Jolla, CA) as previously described (*15*). The protein was purified in the same manner as wild type 2N4R htau (above).

Polymerization Reaction. Tau polymerization was induced by incubating the protein (4 μM, unless otherwise indicated) in the presence of 75 μM arachidonic acid (AA) in buffer containing 50 mM HEPES, pH 7.64, 50 mM NaCl, 0.1 mM EDTA, and 5 mM DTT. The addition of arachidonic acid resulted in a final concentration of 3.75% ethanol carrier. Polymerization reactions were performed at room temperature.

Electron Microscopy. Aliquots for electron microscopy were taken from polymerization reactions after 5 h and fixed with 2% glutaraldehyde for 15 min. Samples were prepared for electron microscopy by floating a carbon-coated Formvar grid on 10 μL of sample for 1 min followed by staining with 2% uranyl acetate for 1 min. A JEOL 1220 transmission electron microscope operating at 60 kV was used to view the grids. Images for quantitation were captured at 20000× using a MegaPlus Model 1.6I AMT Digital Kodak camera controlled by the AMT Camera Controller software package. Five fields of view were blindly selected from the grid for processing. All images were processed and quantified as previously described (*13*, *14*).

Length Distributions. Digital electron micrographs were imported into the Optimas 6.1 software package (Media Cybernetics) that was used to automatically trace a line along the length of individual filaments. Filament lengths were then extracted into GraphPad Prism software where the relative frequencies of individual filament lengths were determined in bins of 100 nm. The number of filaments in each bin was multiplied by the value of the bin in order to estimate the overall mass of filaments that fell into each bin.

Laser Light Scattering. Laser light scattering measurements of tau polymerization reactions were performed as described previously (*14*). Briefly, tau polymerization reactions (250 μL) in 5 mm fluorometer cells were illuminated with 488 nm vertically polarized laser light generated by a Lexel Model 65 ion laser at a 5 mW setting. Images were collected at an angle of 90° to the incident light and perpendicular to the direction of polarization with an Electrim Corp. Model EDC1000HR digital camera with a 25 mm lens controlled by HiCam '95 (written by Dr. Guenter Albrecht-Buehler of Northwestern University Medical School and available at http://www.basic.northwestern.edu/g-buehler/hicam.htm). The intensity of scattered light (i_s) was obtained using the histogram feature of Adobe Photoshop. The data were fit to simple association equations using GraphPad Prism software.

RESULTS

The involvement of the amino terminus of the tau molecule in its polymerization was investigated by using two different mutant forms of the protein (Figure 1). The first mutant employed lacked amino acids 2−18 (*21*). The second construct was generated by site-directed mutagenesis to create the recently described FTDP-17 mutant of tau, $^{R}5^{L}$ (*23*).

Polymerization reactions were performed with the N-terminal variants using wild-type protein as a control. Wild-type tau protein was induced to form filaments in the presence of arachidonic acid as assayed by negative stain electron microscopy (Figure 2, top panel). The filaments had morphologies similar to straight filaments observed in

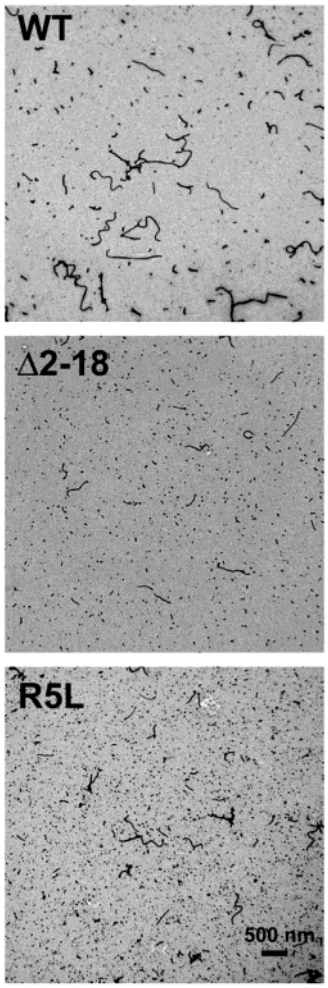

FIGURE 2: Effects of amino-terminal modification on the morphology of tau filaments. Tau filaments generated from wild-type tau (top panel, WT), the Δ2−18 construct (middle panel, Δ2−18), and $^{R}5^{L}$ (bottom panel, R5L) at a concentration of 4 μM were viewed by negative stain electron microscopy at a magnification of 20000×. Representative digital micrographs are shown here. The size bar represents 500 nm.

Alzheimer's disease and other neurodegenerative disorders, as has been reported previously (*12*). The filaments that resulted from the addition of arachidonic acid to solutions of Δ2−18 were qualitatively different from those formed by wild-type tau (Figure 2, middle panel). Although the addition of arachidonic acid does induce polymerization, the resulting filaments appear to be shorter in length than those formed by wild-type tau. The addition of arachidonic acid to solutions of the $^{R}5^{L}$ mutant resulted in filaments that were qualitatively different from those of wild-type protein (Figure 2, bottom panel). As was the case with Δ2−18, the $^{R}5^{L}$ filaments appeared to be shorter than those formed by wild-type protein.

The qualitative assessments of filament morphologies were confirmed by quantitative analysis of filament lengths (Figure 3). Wild-type filaments were found to have lengths up to 1750 nm, with approximately 24% of the filament mass consisting of filaments with lengths of 0−100 nm. Δ2−18 filaments were found to have lengths up to 850 nm, with approximately 74% of the filament mass being filaments with lengths below 100 nm. $^{R}5^{L}$ filaments were also found to be much shorter than wild-type filaments, with approximately 81% of the filament mass resulting from filaments with

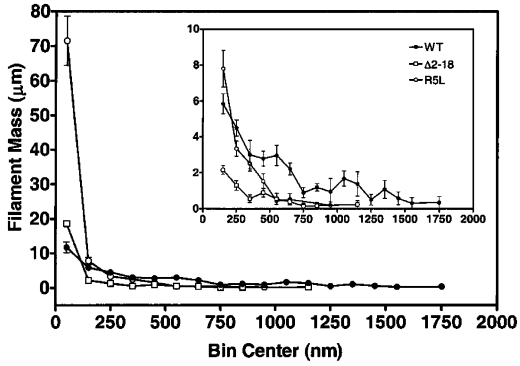

FIGURE 3: Frequency distributions of polymer mass by length. Frequency distributions of the filament lengths formed by wild-type tau (closed circles), Δ2−18 (open squares), and $^{R}5^{L}$ (open circles) were determined using an automatic "find lines" feature of the Optimas software package. Histograms were generated using GraphPad software and a bin size of 100 nm (the center of the first bin is 50 nm). The number of filaments that fell into each bin (n_i) were multiplied by the bin center (L_i) to approximate the mass of filaments in each bin ($\sum\mu$m). Data points are the average mass of filaments in each bin (±1 SEM) as determined from five different fields of view at 20000×, similar to those shown in Figure 2. The inset is the same data without the first data point and on a different scale to better show the differences in filament length distributions.

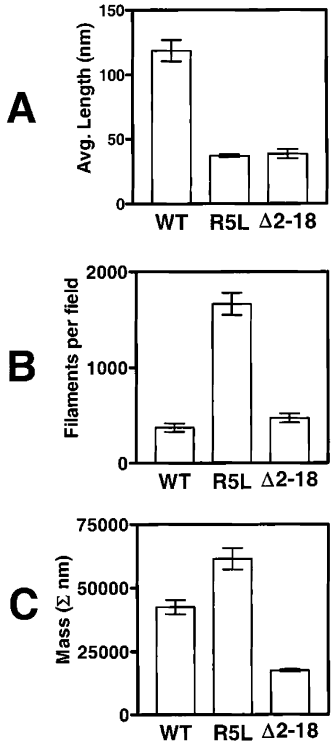

FIGURE 4: Quantitative electron microscopy measurements of amino-terminal modifications. (A) The average length of filaments per field of view (±SEM) at a magnification of 20000× was measured for each protein (*x*-axis). (B) The average number of the filaments per field of view measured in (A) is depicted here for each protein (*x*-axis). (C) The average number of filaments was multiplied by the average length of filaments to obtain the average mass of filaments in each field (±SEM) for each protein (*x*-axis).

lengths of 0−100 nm. These differences in filament length distributions resulted in a large difference between the average filament lengths for the three constructs, with wild-type filaments having an average length more than double that of $^{R}5^{L}$ and Δ2−18 (Figure 4A). However, the $^{R}5^{L}$ modification of tau resulted in a 4.5-fold increase in the

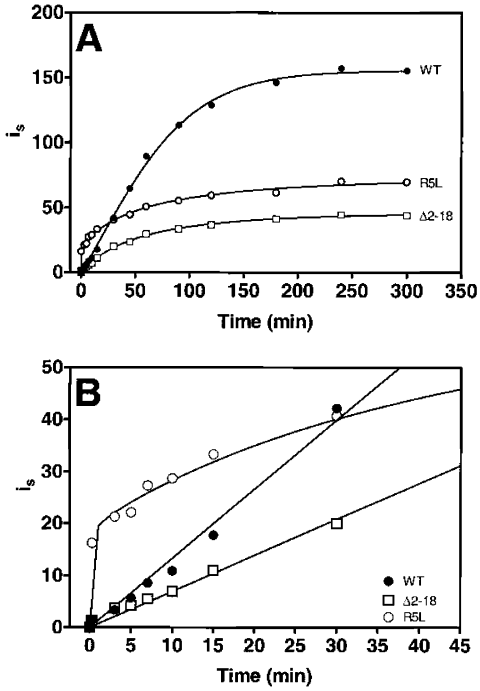

FIGURE 5: Amino-terminal modification alters the apparent kinetics of tau polymerization. Polymerization reactions were performed at room temperature in the presence of 75 μM arachidonic acid and 4 μM wild-type tau (closed circles), $^{R}5^{L}$ (open circles), or Δ2−18 (open squares). The reactions were monitored using right angle laser light scattering (LLS). The intensity of scattered light (i_s) was measured at various time points over the course of 6 h. (A) Entire polymerization reactions from representative experiments are illustrated. The data are fit to a two-phase hyperbolic equation. (B) The early time points (first 45 min) from the data for wild-type tau (closed circles) and the Δ2−18 construct (open squares) illustrated in (A) are redrawn here and fit to a linear regression in order to determine the approximate initial velocities of the reactions. The early time points for $^{R}5^{L}$ (open circles) are also redrawn and fit to a two-phase equation.

number of filaments generated as compared to wild-type tau and Δ2−18 (Figure 4B). When these measurements are combined, the $^{R}5^{L}$ mutation results in the generation of 1.4 times more polymer mass than wild-type tau (Figure 4C). Additionally, the removal of the amino terminus (Δ2−18) results in a 2.4-fold reduction in polymer mass as compared to wild-type tau using this same technique (Figure 4C).

The length distributions for the $^{R}5^{L}$ and Δ2−18 mutations suggested that laser light scattering would not be a useful tool for monitoring the mass of filaments formed. Since a large proportion of the filaments are shorter than one-sixth the wavelength of light employed (or approximately 80 nm), they are not efficient scattering particles (*24*). Laser light scattering experiments confirmed this prediction (Figure 5A). Polymerization reactions with the $^{R}5^{L}$ mutant generated less laser light scattering than wild-type protein. The Δ2−18 mutant generated less laser light scattering than both wild type and the $^{R}5^{L}$ mutant, further reinforcing the prediction that the short filaments generated are not efficient scattering particles. Although these measurements are likely only measuring approximately 26% and 19% of the filament mass for Δ2−18 and the $^{R}5^{L}$ mutant, respectively, they do report the relative speed with which these particles appear. Linear regression analysis of the early changes in polymerized material revealed that the Δ2−18 construct polymerized with an apparent initial velocity 50% slower than that of wild-type tau (Figure 5B). In contrast, the $^{R}5^{L}$ mutant demonstrated a very rapid initial increase in scattering (Figure 5B), indicating that the polymerization process for the $^{R}5^{L}$ mutant is more efficient than for wild type or the Δ2−18 mutant.

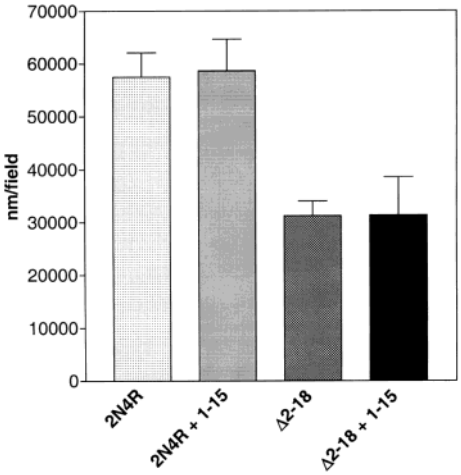

FIGURE 6: Adding back 1−15 peptide does not influence tau polymerization. Tau polymerization reactions were performed, utilizing wild-type protein and Δ2−18 protein at concentrations of 4 μM in the presence or absence of 100 μM peptide corresponding to amino acids 1−15 of the tau molecule. The reactions were incubated for 5 h, and samples were removed and processed for negative stain electron microscopy. The sum of the lengths of the filaments in a field at a magnification of 20000× was quantified to estimate the mass of filaments formed. Five blindly selected fields were measured for each condition, and the average ± SEM in units of nanometers is reported.

Since these results suggested that tau's amino terminus facilitates polymerization, it was of interest to ask whether this effect might be mimicked by a synthetic peptide corresponding to this region (residues 1−15). Such a peptide was added at a concentration of 100 μM to polymerization reactions consisting of 4 μM wild-type tau or Δ2−18. Quantitation by electron microscopy demonstrated no difference in polymer mass for either protein or in the presence or absence of the peptide (Figure 6).

DISCUSSION

The tau pathology in Alzheimer's disease has been shown to consist of filamentous structures that possess a protease-resistant "core". The region of tau present in this core roughly corresponds to the microtubule-binding repeat regions (MTBR) (*25*). Therefore, it can be surmised that this region of tau is involved in the polymerization process. In support of this, the third microtubule-binding repeat has been shown to be essential for the in vitro polymerization of tau in two separate polymerization paradigms. The region ^{314}DLSKVTS^{320} has been shown to be essential for the fatty acid induction of tau polymerization (*17*), while an adjoining region, ^{306}VQIVYK^{311}, has been shown to be essential for the polyanionic induction of tau polymerization (*18*). These results strengthen the case for the central role of the microtubule-binding repeats in tau's polymerization.

Although the PHF core is present in all pathological tau structures, there is an abundance of data demonstrating the inclusion of intact protein in these structures in addition to various truncated forms (*26*). Therefore, the question remains as to how regions outside of the vital microtubule-binding repeat region can influence tau polymerization. This report

clearly demonstrates that the alteration or removal of tau's amino terminus can modify its ability to polymerize. Both the rate and extent of polymerization can be affected by these modifications, suggesting a role for the amino terminus in the molecular mechanism of tau polymerization.

Other regions of the tau molecule outside the microtubule-binding repeats have also been shown to influence its polymerization. The carboxyl terminus of tau has been shown to negatively regulate the polymerization process. It has been postulated that this region of the molecule folds over to make an interaction with the MTBR in order to adopt an inhibitory conformation (*17*). This view is supported by the evidence that the third MTBR and the carboxy-terminal tail map as two of the most hydrophobic regions of the molecule. The hydrophobicity of the carboxyl terminus is likely enhanced by the adoption of α-helical structure (*27*), which is predicted to be amphipathic by helical wheel analysis (unpublished observation). Given the highly flexible nature of the tau molecule, it is not unreasonable that these two regions could interact with one another.

A similar conformation can be postulated for the amino terminus. Mapping of the Alz50 epitope has shown that the extreme amino terminus is capable of interacting with the microtubule-binding repeat region of tau (*19*−*21*). The adoption of this conformation is thought to precede tau polymerization (*22*). The results in this report support the supposition that the Alz50 conformation enhances the ability of tau to polymerize, in that the removal of the extreme amino terminus, which precludes the adoption of the Alz50 conformation, reduces both the rate and extent of tau polymerization. At first glance, the fact that Δ2−18 forms the same number of filaments as wild type, but shorter ones, would seem to imply that residues 2−18 primarily affect filament elongation, rather than nucleation. However, this remains to be tested directly.

It is tempting to speculate that the amino- and carboxy-terminal regions of tau are competing for the same region of the MTBR, but the current data do not support such a view. As mentioned above, sequence analysis suggests that the interaction between the carboxyl terminus and the MTBR is likely hydrophobic in nature. The amino terminus does not share this hydrophobic nature, and unlike the carboxyl terminus, the amino terminus does not appear to adopt α-helical structure in 36% trifluoroethanol (unpublished observation). Sequence analysis of the amino terminus reveals few striking characteristics. However, the first 25 amino acids do have a net charge of −4 while the third MTBR has a net charge of +3. Although this might only provide a weak electrostatic interaction, it is possible that such a mechanism could be responsible for their association. Since the $^{R}5^{L}$ mutation presumably enhances this association, clues about the interaction can be obtained from the change in sequence provided by $^{R}5^{L}$. The first change is that the overall charge of this region would be changed from −4 to −5, possibly strengthening the electrostatic interaction between the two regions. Another change would be to make the amino terminus more hydrophobic and, therefore, more similar to the third MTBR. It is perhaps the combination of these two changes that provides such an increase in polymerization for the $^{R}5^{L}$ mutant.

It is likely that tau in solution exists in many different conformational states. This conformational flux arises from the dynamic equilibrium between the different conformations made possible by the high flexibility of the tau molecule. Such a dynamic equilibrium could be partly responsible for the relative absence of tau secondary structure in solution, since many of the adopted conformations would be transient and, therefore, difficult to measure with current technologies. The results from this report and previously published data suggest that at least two major conformational states of tau exist. The first is that of an inhibitory conformation, with the carboxyl terminus folding over to make a hydrophobic interaction with the MTBR (Figure 7). The second is a "propolymerization" conformation, with the amino terminus folding over to make an electrostatic interaction with the MTBR (Figure 7). It is reasonable to assume that the interaction that each of these two regions has with the MTBR is different from one another. If the nature of their interaction with the MTBR were similar, it would be expected that the functional consequence of their association with the MTBR would also be similar. It is likely that, in the case of the amino-terminal interaction, it is the conformation of the molecule that is responsible for the enhancement of polymerization, rather than the simple association of the two regions. The addition of an excess of peptide corresponding to the amino terminus, which is free to interact with the MTBR, does not affect polymerization. This result decreases the possibility that a simple association between the MTBR and the amino terminus is sufficient to enhance polymerization but rather supports the supposition that the specific torsion of the molecule required to make the association drives polymerization. The notion of a specific torsional strain on the tau molecule is supported by previous work (*13*) in which deletion of exons 2 and 3 between the amino terminus and microtubule-binding repeat regions had a seemingly negative effect on tau polymerization. Future experimentation will be performed to ascertain whether the $^{R}5^{L}$ mutation is capable of rescuing the polymerization of these isoforms of tau.

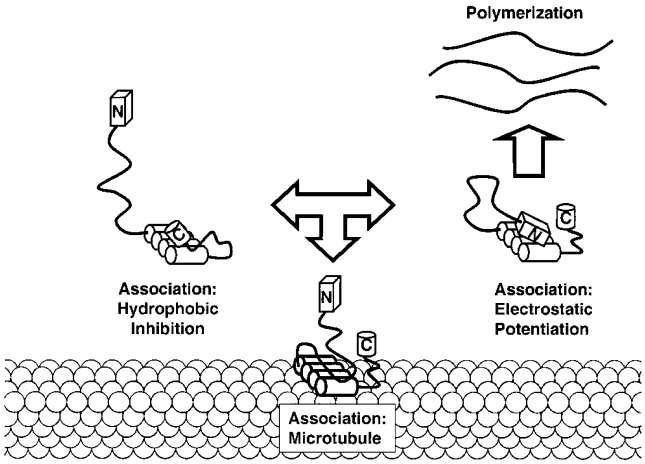

FIGURE 7: Schematic of inhibitory and propolymerization conformations of tau. This schematic depicts the tau molecule with four microtubule-binding repeats (cylinders), a carboxyl terminus (cylinder labeled "C"), and an amino terminus (block labeled "N"). The amino and carboxyl termini of tau are connected to the microtubule-binding repeats by very flexible regions of tau. In this model, these flexible regions allow for the carboxyl terminus to interact with the microtubule-binding repeats and inhibit tau polymerization and also allow for the interaction of the amino terminus with the microtubule-binding repeats, which is stimulatory for tau polymerization. See text for details.

Given the highly flexible nature of tau, it is likely that the schematic in Figure 7 is a simplification of the number of possible conformations. However, it is clear that changes to the tau molecule that alter the conformational dynamic equilibrium also have a large impact on its polymerization. For example, the pseudophosphorylation of tau at serine 396 and serine 404 leads to an increase in polymerization. Using this model, it would be predicted that this modification reduces the occurrence of the inhibitory conformation since the modification lies in a flexible region between the MTBR and the carboxyl terminus. If phosphorylation at these sites reduced the flexibility of this region, it could significantly alter the amount of time spent in the inhibitory conformation, shifting the dynamic equilibrium toward the propolymerization conformation. Likewise, the $^{R}5^{L}$ mutation could enhance the amino-terminal−MTBR interaction, effectively shifting the dynamic equilibrium toward the propolymerization conformation. Therefore, another prediction arising from this model is that other changes in the flexible regions between the MTBR and the interacting termini should also influence the conformational dynamic equilibrium of tau.

Conclusions. We have shown that the amino terminus of tau can play an important role in regulating its polymerization in vitro. The interaction of the amino terminus of tau with its MTBR, creating a conformation similar to that recognized by the monoclonal antibody Alz50, is very likely a propolymerization state of the tau molecule. Therefore, the inhibition of this interaction is a potential therapeutic target for decreasing the amounts of abnormally polymerized tau in neurodegenerative disease.

ACKNOWLEDGMENT

We thank Matt Anderson for generating the $^{R}5^{L}$ construct. We thank Dr. Robley C. Williams, Jr., for helpful suggestions during the preparation of the manuscript.

REFERENCES

1. Lee, V. M., Goedert, M., and Trojanowski, J. Q. (2001) *Annu. Rev. Neurosci. 24*, 1121−1159.
2. Arriagada, P. V., Growdon, J. H., Hedley-Whyte, E. T., and Hyman, B. T. (1992) *Neurology 42*, 631−639.
3. Wilson, D. M., and Binder, L. I. (1995) *J. Biol. Chem. 270*, 24306−24314.
4. Goedert, M., Jakes, R., Spillantini, M. G., Hasegawa, M., Smith, M. J., and Crowther, R. A. (1996) *Nature 383*, 550−553.
5. Friedhoff, P., Schneider, A., Mandelkow, E. M., and Mandelkow, E. (1998) *Biochemistry 37*, 10223−10230.
6. Arrasate, M., Perez, M., Armas-Portela, R., and Avila, J. (1999) *FEBS Lett. 446*, 199−202.
7. Goedert, M., Jakes, R., and Crowther, R. A. (1999) *FEBS Lett. 450*, 306−311.
8. Hasegawa, M., Crowther, R. A., Jakes, R., and Goedert, M. (1997) *J. Biol. Chem. 272*, 33118−33124.
9. Nacharaju, P., Lewis, J., Easson, C., Yen, S., Hackett, J., Hutton, M., and Yen, S. H. (1999) *FEBS Lett. 447*, 195−199.
10. Perez, M., Valpuesta, J. M., Medina, M., Montejo de Garcini, E., and Avila, J. (1996) *J. Neurochem. 67*, 1183−1190.
11. Kampers, T., Friedhoff, P., Biernat, J., Mandelkow, E. M., and Mandelkow, E. (1996) *FEBS Lett. 399*, 344−439.
12. King, M. E., Ahuja, V., Binder, L. I., and Kuret, J. (1999) *Biochemistry 38*, 14851−14859.
13. King, M. E., Gamblin, T. C., Kuret, J., and Binder, L. I. (2000) *J. Neurochem. 74*, 1749−1757.
14. Gamblin, T. C., King, M. E., Dawson, H., Vitek, M. P., Kuret, J., Berry, R. W., and Binder, L. I. (2000) *Biochemistry 39*, 6136−6144.
15. Gamblin, T. C., King, M. E., Kuret, J., Berry, R. W., and Binder, L. I. (2000) *Biochemistry 39*, 14203−14210.
16. Wilson, D. M., and Binder, L. I. (1997) *Am. J. Pathol. 150*, 2181−2195.
17. Abraha, A., Ghoshal, N., Gamblin, T. C., Cryns, V., Berry, R. W., Kuret, J., and Binder, L. I. (2000) *J. Cell Sci. 113*, 3737−3745.
18. von Bergen, M., Friedhoff, P., Biernat, J., Heberle, J., and Mandelkow, E. (2000) *Proc. Natl. Acad. Sci. U.S.A. 97*, 5129−5134.
19. Jicha, G. A., Berenfeld, B., and Davies, P. (1999) *J. Neurosci. Res. 55*, 713−723.
20. Jicha, G. A., Lane, E., Vincent, I., Otvos, L., Jr., Hoffmann, R., and Davies, P. (1997) *J. Neurochem. 69*, 2087−2095.
21. Carmel, G., Mager, E. M., Binder, L. I., and Kuret, J. (1996) *J. Biol. Chem. 271*, 32789−32795.
22. Tabaton, M., Whitehouse, P. J., Perry, G., Davies, P., Autilio-Gambetti, L., and Gambetti, P. (1988) *Ann. Neurol. 24*, 407−413.
23. Poorkaj, P., Muma, N. A., Zhukareva, V., Cochran, E. J., Shannon, K. M., Hurtig, H., Koller, W. C., Bird, T. D., Trojanowski, J. Q., Lee, V. M., and Schellenberg, G. D. (2002) *Ann. Neurol. 52*, 511−516.
24. Berne, B. J. (1974) *J. Mol. Biol. 89*, 755−758.
25. Wischik, C. M., Novak, M., Thogersen, H. C., Edwards, P. C., Runswick, M. J., Jakes, R., Walker, J. E., Milstein, C., Roth, M., and Klug, A. (1988) *Proc. Natl. Acad. Sci. U.S.A. 85*, 4506−4510.
26. Ghoshal, N., Garcia-Sierra, F., Wuu, J., Leurgans, S., Bennett, D. A., Berry, R. W., and Binder, L. I. (2002) *Exp. Neurol. 177*, 475−493.
27. Esposito, G., Viglino, P., Novak, M., and Cattaneo, A. (2000) *J. Pept. Sci. 6*, 550−559.

BI0272510